Shape Complementarity, Binding-Site Dynamics, and Transition State Stabilization: A Theoretical Study of Diels–Alder Catalysis by Antibody 1E9

Jiangang Chen,[a] Qiaolin Deng,[a] Renxiao Wang,[a] Kendall N. Houk,*[a] and Donald Hilvert*[b]

Antibody 1E9 is a protein catalyst for the Diels–Alder reaction between tetrachlorothiophene dioxide and N*-ethylmaleimide. Quantum mechanical calculations have been employed to study the 1E9-catalyzed Diels–Alder reaction in the gas phase. The transition states and intermediates were all determined at the B3LYP/6-31G*//HF/6-31G* level. The cycloaddition step is predicted to be rate-determining, and the* endo *reaction pathway is strongly favored. Binding of the reactants and the transition states to antibody 1E9 was investigated by docking and molecular dynamics simulations. The linear interaction energy (LIE) method was adopted to estimate the free energy barrier of the 1E9-catalyzed Diels–Alder reaction. The catalytic efficiency of antibody 1E9 is achieved by enthalpic stabilization of the transition state, near-perfect shape complementarity of the hydrophobic binding site for the transition state, and a strategically placed hydrogen-bonding interaction.*

KEYWORDS:

catalytic antibodies · Diels–Alder reactions · molecular docking · molecular dynamics · protein–ligand interactions · transition states

Introduction

The Diels–Alder reaction is one of the most useful carbon–carbon-bond-forming transformations in organic chemistry.[1] This process involves the concerted [4+2] cycloaddition of a diene to a dienophile and occurs via a highly ordered cyclic transition state. Although no enzyme for such a reaction has been well characterized,[2] several groups have produced antibodies that catalyze Diels–Alder reactions.[3–6] Cycloadditions represent challenging targets for catalysis since there are no ionic intermediates and little charge separation in the transition state. Therefore, shape complementarity must be maximally exploited for eliciting effective catalysts.

Antibody 1E9 was the first antibody catalyst for a Diels–Alder reaction.[7] It catalyzes the cycloaddition between tetrachlorothiophene dioxide (**1**) and *N*-ethylmaleimide (**2**) (Scheme 1). This reaction proceeds in two steps: The cycloaddition gives intermediate **3**, which eliminates sulfur dioxide to give product **4**. The latter subsequently undergoes air oxidation to form *N*-ethyl tetrachlorophthalimide (**5**). Antibody 1E9 was raised against the hexachloronorbornene derivative **6a** (R = $(CH_2)_5COO^-$, Scheme 1) which is an excellent structural analogue of the unstable intermediate and its flanking transition states. Product inhibition is effectively minimized since the planar product is structurally very different from the transition state. As judged by k_{cat}/k_{uncat} values of 1000 M,[8a] 1E9 is significantly more efficient than other antibodies in catalyzing Diels–Alder reactions.

Unexpectedly, the experimentally determined entropy of the 1E9-catalyzed reaction is essentially the same as that of the uncatalyzed reaction in water. From the temperature dependence of k_{cat}, values for the enthalpy and entropy of activation for the 1E9-catalyzed reaction of 11.3 kcal mol^{-1} and -22.1 entropy units (e.u.; 1 e.u. = 1 cal K^{-1} mol^{-1}), respectively, can be derived. The corresponding values for the uncatalyzed reaction are 15.5 kcal mol^{-1} and -21.5 e.u.[8a] The lowered barrier of the 1E9-catalyzed reaction thus comes mainly from the enthalpic stabilization of the transition state.

The crystal structure of 1E9 complexed with a hapten molecule has been resolved at 1.9 Å resolution.[8a] This structure reveals a binding pocket pre-organized to maximize the shape complementarity with the hapten (Figure 1). Ligand recognition

[a] *Prof. K. N. Houk, J. Chen, Q. Deng, R. Wang*
Department of Chemistry and Biochemistry
University of California
Los Angeles, CA 90095-1569 (USA)
Fax: (+1) 310-206-1843
E-mail: houk@chem.ucla.edu

[b] *Prof. D. Hilvert*
Laboratory of Organic Chemistry
ETH Zentrum
8092 Zürich (Switzerland)
Fax: (+41) 1-632-1486
E-mail: hilvert@org.chem.ethz.ch

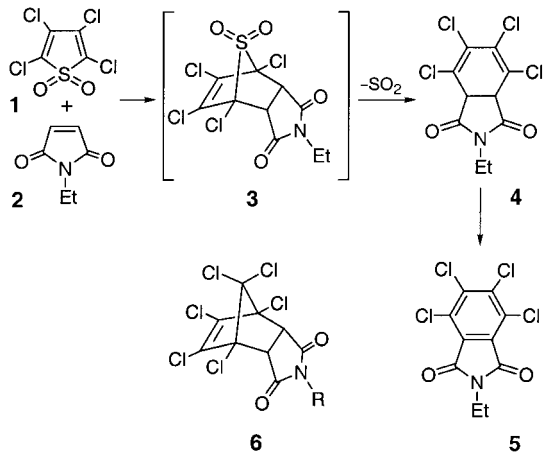

Scheme 1. *1E9-catalyzed Diels–Alder reaction. See text for details and Table 1 for the different side chains R of hapten* ***6****.*

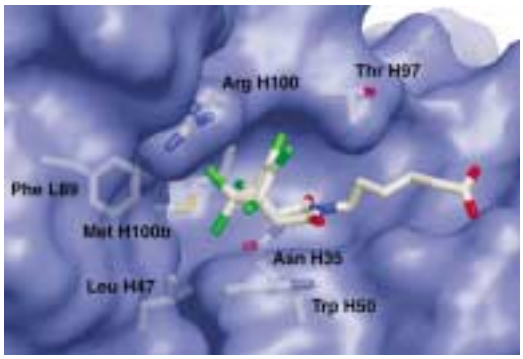

Figure 1. *Binding site of the 1E9–hapten complex as determined by X-ray structure analysis.*[8a]

Editorial Advisory Board Member:[*]
Donald Hilvert

is Professor of Chemistry at the Swiss Federal Institute of Technology (ETH). He received a Ph.D. in chemistry from Columbia University, New York, in 1983. After postdoctoral studies at Rockefeller University, New York, he joined the faculty of the Scripps Research Institute in La Jolla, California, where he pursued his interests in chemical biology. In 1997 he moved to Switzerland and assumed his current position. His research program focuses on understanding how enzymes work and on mimicking the properties of these remarkable catalysts in the laboratory. These efforts have been recognized by a number of awards, including the Pfizer Award in Enzyme Chemistry.

[*] *Members of the Editorial Advisory Board will be introduced to the readers with their first manuscript.*

is achieved through van der Waals contacts of the hexachloronorbornene moiety with multiple aliphatic and aromatic residues. Notable in this regard is the π-stacking interaction between the succinimide group of the hapten, which corresponds to the maleimide substrate, and the indole ring of Trp H50. The only polar residue in the binding pocket is the highly conserved Asn H35, which donates a hydrogen bond to the more deeply buried succinimide carbonyl group.

Although the crystal structure provides a qualitative picture of how 1E9 binds the hapten, explaining the origin of catalysis requires a quantitative calculation. Here we present a detailed computational study of 1E9 that illuminates the function and selectivity of this antibody. We have also examined the role of dynamic motion of the antibody. Our results have revealed that transition state stabilization comes from excellent shape and chemical complementarity between the binding pocket and the transition state.

Computational Methods

Quantum mechanical calculations: All quantum mechanical calculations were performed with the Gaussian 94 program.[9] Stationary points along the reaction pathway corresponding to reactants **1** and **2**, the cycloaddition transition state, intermediate **3**, and the transition state for sulfur dioxide elimination were determined by optimizations with Hartree–Fock calculations and the 6-31G* basis set, followed by hybrid density functional B3LYP calculations (B3LYP/6-31G*//HF/6-31G*). Subsequent frequency and intrinsic reaction coordinate (IRC) calculations verified that all the transition states were first-order saddle points. Both the *endo* and *exo* reaction pathways were studied.

Docking studies: We explored the binding of a reactant complex, the transition states, and the haptens of both the *endo* and *exo* reaction pathway to antibody 1E9. All docking calculations were performed with the AutoDock 3.0 program.[10] This program predicts the binding of a flexible ligand molecule to a rigid macromolecular receptor. It uses a genetic algorithm to sample conformational space and a grid-based method for force field energy evaluation. An empirical function is also implemented to estimate the free energy of binding. In our docking studies, the crystal structure of antibody 1E9 complexed with the hapten was used. All the rotatable single bonds on the ligand molecules were allowed to rotate. The electrostatic-potential-derived charges calculated with the Merz–Kollman method were assigned for docking calculations.[11] All the other parameters relied on the default values provided by the AutoDock program. The lowest energy binding modes of ligand molecules were determined through the cluster analysis provided by AutoDock.

Molecular dynamics simulations and free energy calculations: We computed the free energy barrier of the 1E9-catalyzed Diels–Alder reaction by using a thermodynamic cycle (Scheme 2). In this scheme, S and TS represent the substrate and the corresponding transition state, respectively, and Ab represents the catalytic antibody. According to this cycle, the difference in the free energy barrier between the uncatalyzed and the catalyzed reaction ($\Delta G_1 - \Delta G_2$) equals the difference in the free energy of binding between the reactant and the transition state ($\Delta G_3 - \Delta G_4$). Therefore, by comparing the free energies of binding of the reactant and the transition state to 1E9, we can compute the acceleration of the reaction by the antibody.

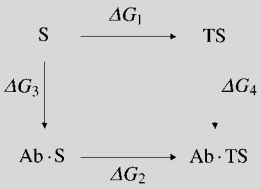

Scheme 2. *Thermodynamic cycle relating the catalyzed and uncatalyzed reactions.*

The free energies of binding were computed with the Linear Interaction Energy (LIE) method.[12–14] The LIE method estimates the free energy of binding by a linear combination of the differences between the averaged ligand–environment interaction energies for the bound and unbound states, as shown in Equation (1).

$$\Delta G_{bind} = \alpha\{\langle V_{bound}^{vdW}\rangle - \langle V_{free}^{vdW}\rangle\} + \beta\{\langle V_{bound}^{elec}\rangle - \langle V_{free}^{elec}\rangle\} \quad (1)$$

Here the free energy of binding is dissected into van der Waals (vdW) and electrostatic (elec) contributions. The terms $\langle V_{free}\rangle$ and $\langle V_{bound}\rangle$ refer to the ensemble-averaged energies for the free state (in aqueous solution) and the bound state (to the protein), respectively. Therefore, two sets of molecular dynamics (MD) simulations are required for an LIE calculation: one for the free ligand in water and the other for the bound ligand with the protein. The ensemble-averaged energy components can be determined from the MD trajectories. According to the LIE method, the electrostatic scaling factor, β, of 0.5 comes from the linear response approximation.[12] The van der Waals scaling factor, α, is usually determined empirically by fitting to the experimental binding data. In our study, we adopted the α value of 0.657 from a previous study of the binding affinities of steroids to antibody DB3.[15] The rationale for doing so comes from the high homology in amino acid sequence and cross-reactivity exhibited between 1E9 and DB3.[16]

We have performed LIE calculations for a reactant complex, the transition state, and the intermediate of the *endo* reaction pathway. Binding of the *endo* hapten to 1E9 was also calculated. The MD simulations were carried out with the AMBER 4.1 program.[17] For simulations in aqueous solution, the ligand was placed in a periodic box of 400 TIP3P water molecules. A residue-based cutoff value of 10 Å for noncovalent interactions was employed. For the simulation of the antibody–ligand complex, the structure predicted by AutoDock was used as the starting conformation. A spherical 20 Å cap of TIP3P water molecules centered at the ligand molecule was added, and a harmonic force constant of 1.5 kcal mol^{-1} Å^{-2} was applied to any water leaving the 20 Å boundary. Only residues within 14 Å of the ligand molecule were allowed to be flexible whereas the other residues were fixed. For all of these calculations, an all-atom AMBER force field was applied, and the SHAKE algorithm was used to constrain bond lengths. The MD trajectories included 40 ps of equilibration and 60 ps of data collection after the initial minimization and heating. The simulations were performed with a time step of 1 fs.

Results and Discussion

The hapten molecule observed in the 1E9 crystal structure has the *endo* configuration. To gain some insight into the importance of shape complementarity for molecular recognition in this system, we have docked both the *endo* and the *exo* hapten molecules into the binding pocket of the antibody. A series of compounds with side chains of variable length was also studied to learn whether the flexible aliphatic side chain influences the docking results. The side chain was varied from a single methyl group (**6 f**) to the hexanoic acid of the original hapten molecule (**6 a**). All the docking results are summarized in Table 1.

For the *endo* hapten series, AutoDock successfully reproduces the binding mode revealed in the crystal structure (Figure 1). Irrespective of side chain length, the hapten always favors this binding mode with 1E9. The important residues for 1E9–hapten interactions include Asn H35, which forms a hydrogen bond to the carbonyl group on the succinimido moiety, and Trp H50, which provides π-stacking interactions with the *endo* hapten. Although the docking orientation does not change, the free energy of binding becomes more favorable with longer side chains. This reflects the shape complementarity between the hapten and the binding cavity. For the *exo* hapten series, the binding mode changes as the side chain varies. Several different low-energy conformation clusters are observed in each case, suggesting that the *exo* hapten does not bind to antibody 1E9 in a specific way. The predicted free energy of binding of the *exo* hapten is also less favorable than that of its *endo* counterpart. The binding site of 1E9 thus accommodates the *endo* hapten better than the *exo* one.

We have further quantified the shape complementarity between the hapten and the 1E9 binding pocket by determining a gap index.[8a] The gap index is defined as the gap volume between antibody and hapten (in Å^3) divided by the buried surface of the hapten (in Å^2). The gap index for the 1E9–hapten complex is 0.4 Å, which is substantially lower than that of antibody–protein complexes we have studied before.[8a] This

Table 1. *Results of docking modified haptens **6** into the active site of antibody 1E9.*

Hapten	R	$n_{rot.}$[a]	$n_{clust.}$[b]		$E_{docking}$ [kcal mol^{-1}][c]		$\Delta G_{docking}$ [kcal mol^{-1}][d]	
			endo	*exo*	*endo*	*exo*	*endo*	*exo*
6 a	$(CH_2)_5COO^-$	6	2	8	−15.1	−13.1	−13.0	−11.0
6 b	$(CH_2)_4CH_3$	4	2	7	−13.6	−11.4	−12.1	−9.9
6 c	$(CH_2)_3CH_3$	3	1	6	−13.2	−11.1	−12.0	−10.0
6 d	$(CH_2)_2CH_3$	2	1	5	−12.5	−10.3	−11.7	−9.6
6 e	CH_2CH_3	1	1	4	−11.4	−9.7	−11.6	−9.4
6 f	CH_3	0	1	2	−11.1	−9.7	−11.1	−9.6

[a] Number of rotatable single bonds in the hapten molecule. [b] Number of clusters obtained in ten runs. [c] Lowest docking energy as given by AutoDock. [d] Lowest free energy of binding as given by AutoDock.

attests to the tight fit of the hapten in the binding site, and the excellent shape complementarity achieved by the antibody.

The structures along the *endo* pathway of the Diels – Alder reaction, given by ab initio calculations, are shown in Figure 2. The computed activation barriers show that the cycloaddition between diene and dienophile ($\Delta E_a = 19.4$ kcal mol^{-1}) is the rate-determining step whereas the sulfur dioxide elimination ($\Delta E_a = 2.3$ kcal mol^{-1}) is much faster. The transition state structures for the *endo* and the *exo* cycloaddition pathways are compared in Figure 3. Both processes are synchronous. The lengths of the

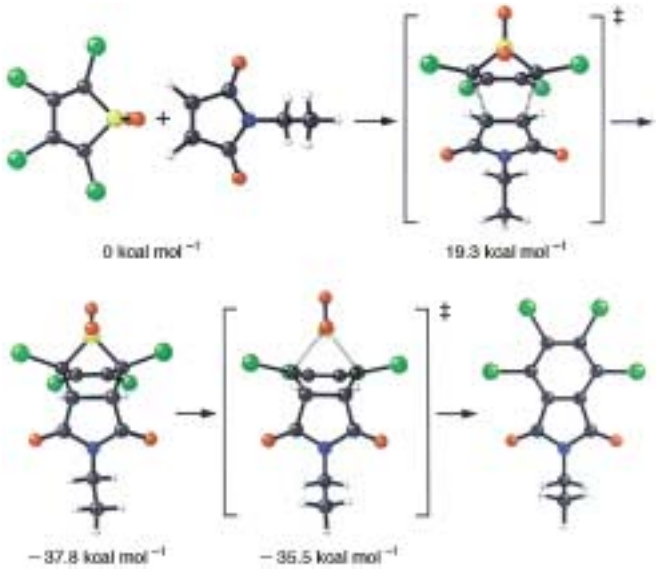

Figure 2. *Pathway and energetics of the 1E9-catalyzed Diels – Alder reaction (B3LYP/6-31G*//HF/6-31G*).*

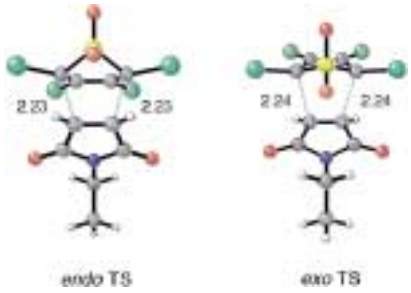

Figure 3. *Comparison of the* endo *and* exo *transition state structures. Distances between reacting atoms are indicated by dashed lines and given in Å.*

forming carbon – carbon bonds between the diene and the dienophile moiety are basically the same for the *endo* (2.23 Å) and the *exo* transition states (2.24 Å). However, the computed activation barrier for the *endo* reaction is 6.9 kcal mol^{-1} lower than for its *exo* counterpart. The large energy difference arises mainly from O-N repulsion in the *exo* transition state.

Both the *endo* and the *exo* transition state models have been docked into 1E9, and a comparison of their binding modes is shown in Figure 4. The dienophile moiety of the *endo* transition state structure overlaps the corresponding part of the docked *endo* hapten very well. In both cases, there is a hydrogen bond

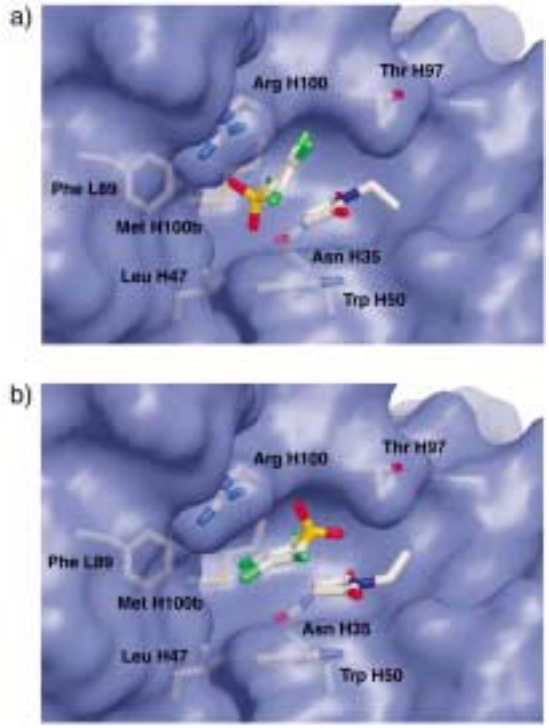

Figure 4. *Transition state models docked inside the binding site. a) The* endo *transition state model; b) the* exo *transition state model.*

between the carbonyl oxygen atom on the dienophile of the transition state structure and the side chain of Asn H35. This hydrogen bond makes the dienophile component more electron-deficient and thus accelerates the Diels – Alder reaction. Because the reaction involves an electron-deficient diene and an electron-deficient dienophile, it should be accelerated by making the dienophile either more electron-deficient—as will occur with hydrogen bonding—or by making it more electron-rich. To examine this point we re-optimized the *endo* transition state model with a water molecule hydrogen-bonded to one carbonyl group. The geometry changes only slightly and the asynchronicity becomes 0.02 Å, but the transition state is stabilized by 0.6 kcal mol^{-1} as compared to the reactant. We also performed a similar calculation for a related Diels – Alder reaction.[8b] For that case, the hydrogen bond increases the asynchronicity by 0.02 – 0.03 Å.

Both transition states exhibit a defined binding mode with an estimated free energy of binding of -10.5 kcal mol^{-1} (given by the AutoDock force field). Considering the considerable difference in the activation barrier of these two reaction pathways in the gas phase, we expect that the *endo* pathway will be highly favored for the catalytic process.

We have also studied the binding of the reactants by using AutoDock. Reactants **1** and **2** have been docked into the 1E9 binding site, and their binding modes are shown in Figure 5. A reactant complex (Figure 5 a) was created by aligning tetrachlorothiophene dioxide (**1**) and *N*-ethylmaleimide (**2**) in a geometry resembling the *endo* transition state, at approximately van der Waals distance. The geometry was chosen so that the sum of the energies of the isolated reactants is the same as the energy of

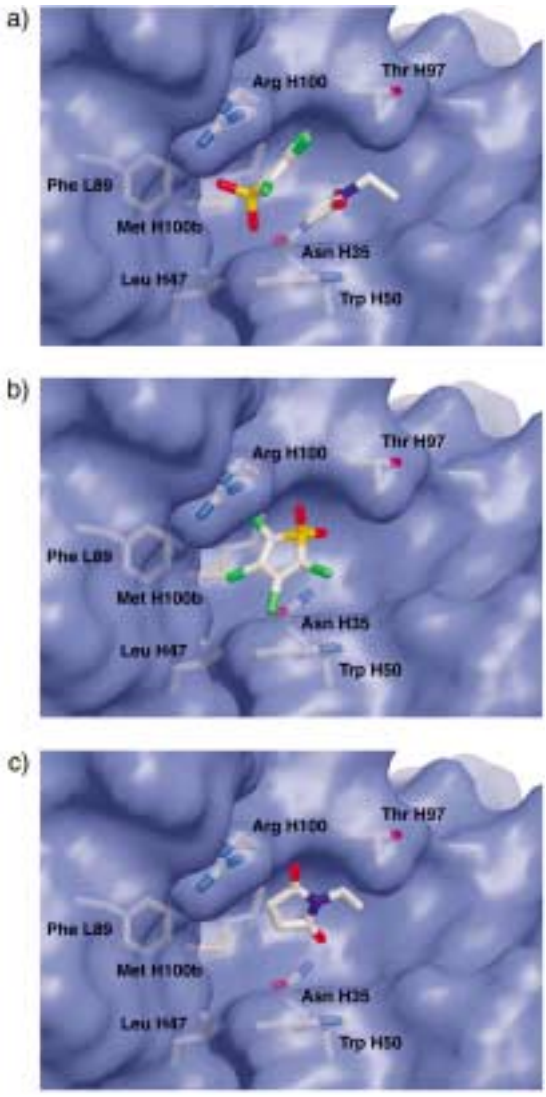

Figure 5. *Binding mode comparison: Reactant complex (a) vs. separately docked reactants (b, diene; c, dienophile).*

this complex. The distance separating the carbon atoms destined to be bonded in the Diels – Alder adduct of the thiophene dioxide and the maleimide are 3.0 Å in this reactant complex. It is obvious that either **1** or **2** will be freer if docked into the binding site alone and, as a result, their binding modes deviate from their counterparts in the reactant complex (Figure 5 b and c). The free energies of binding predicted by AutoDock are -7.1 kcal mol^{-1} and -5.0 kcal mol^{-1} for **1** and **2**, respectively. The total binding energy is about the same as the free energy of binding of the reactant complex (-11.5 kcal mol^{-1}) predicted by AutoDock.

Since AutoDock only gives a rough estimation of free energy of binding (the average error is around 2 kcal mol^{-1}), we have quantified the energetics of the 1E9-catalyzed reaction (*endo* pathway) by more accurate LIE calculations. The results are summarized in Table 2. Note that the scaling factor α in the LIE equation [see Eq. (1)] is usually determined by studying a set of ligand molecules with known free energies of binding. However,

Table 2. *Calculated linear interaction energies.*[a]

Ligand	$\alpha\Delta V^{vdW}$	$\beta\Delta V^{elec}$	ΔG_{bind} [kcal mol^{-1}]
reactant complex	-12.7	6.5	-6.2
transition state	-13.2	4.3	-8.9
intermediate	-13.5	4.5	-9.0
hapten	-13.2	1.5	-11.8

[a] Here $\alpha = 0.657$, $\beta = 0.500$, the free energy of binding is defined as $\Delta G_{bind} = \alpha\Delta V^{vdW} + \beta\Delta V^{elec}$.

establishing a calibration set for antibody 1E9 is not possible yet since only a few binding constants have been measured. Nevertheless, 1E9 is closely related to DB3, an antibody to progesterone.[18] The homology in amino acid sequence between 1E9 and DB3 is over 80 %. Their binding sites are also very similar, as judged by experiments in which 1E9 and DB3 were shown to cross-react with each other's antigen.[16] Therefore, we adopted the scaling factor α from a previous LIE study of DB3 antigens.[15] With this value for α, we have been able to predict a free energy of binding for hapten **6a** of -11.8 kcal mol^{-1}, which is in excellent agreement with the experimental value of -11.4 kcal mol^{-1}.[8a]

According to our LIE results, the free energy of binding of the reactant complex described earlier is -6.2 kcal mol^{-1}. However, there will be an entropy loss upon association of the diene and the dienophile into this loose complex. We estimate this entropy loss to be about 10 e.u.[19] This value corresponds to the elimination of one translational degree of freedom from two organic molecules of average size at 1 M concentration under standard conditions. A similar value has been obtained by Hine,[20] who estimated that the entropy loss upon forming an "intimate encounter complex" is 8 e.u. for substrates in a nucleophilic reaction. The corresponding free energy change has also been called the "cratic free energy", which comes from associating two molecules by restricting translational and rotational freedom.[21] Using this estimate of 10 e.u. for the reactant complexation process (equal to 3.0 kcal mol^{-1} at 298 K), the overall free energy change in binding **1** and **2** to antibody 1E9 is modified from -6.2 kcal mol^{-1} to -3.2 kcal mol^{-1}. The free energy for binding of the transition state is predicted to be -8.9 kcal mol^{-1}, similar to the free energy of binding computed for intermediate **3**, that is -9.0 kcal mol^{-1}. This similarity is not surprising, considering the close structural resemblance of the transition state and compound **3**. Based on these values, the free energy barrier of the 1E9-catalyzed Diels – Alder reaction is lowered by $8.9 - 3.2 = 5.7$ kcal mol^{-1} compared to that of the uncatalyzed reaction. This is in reasonable agreement with the experimental value of 4.0 kcal mol^{-1} obtained with a modified diene.[8a]

The data in Table 2 also provide insight into the molecular basis for the stabilization of the transition state by the antibody. It is obvious that the binding of either the reactant complex or the transition state is dominated by favorable van der Waals interactions, reflecting the hydrophobic nature of the 1E9 binding site. Nevertheless, such interactions provide rather poor discrimination between the reactant complex (-12.7 kcal mol^{-1})

and the transition state (-13.2 kcal mol^{-1}). In contrast, electrostatic interactions become less favorable upon reactant binding but are considerably improved in the transition state, due in part to the increased strength of the hydrogen bond from Asn H35 to the carbonyl group of the dienophile in the transition state.

Gap indices were also calculated for the reactant complex and the transition state. These indices were based on MD-trajectory-averaged coordinates, since X-ray data are, of course, unavailable for these structures. The transition state has a slightly lower gap index (0.7 Å) than the reactant complex (0.9 Å). These computed gap index values are higher than that of the hapten (0.4 Å), the natural ligand for 1E9, but they are significantly lower than the calculated gap index for another antibody catalyzing Diels–Alder reactions, 39A11 (1.69 Å),[8a] indicating excellent shape complementarity with the binding pocket.

We conclude that the tight fit between the antibody and substrates or transition states, relative to water, is responsible for binding, but that the increased electrostatic complementarity of the antibody for the transition state is responsible for catalysis. This conclusion is consistent with results obtained with other enzymes for which free energy calculations have been performed. Namely, enhanced van der Waals interactions favor complexation, but electrostatic interactions in the complex are generally less favorable than in water.[22] Optimization of the latter is essential for truly effective catalysis.[23]

MD simulations, as employed in the LIE calculations, provide additional evidence for the origin of the catalytic efficiency of 1E9. During each MD simulation, the root-mean-square deviation (RMSD) of each residue from the average structure observed in the MD trajectories was calculated. The RMSD value was calculated by using all heavy atoms in a residue, and it provides a measure of residue flexibility. Figure 6 shows the RMSD values of each residue in the MD simulations. Some residues have zero RMSD values because they are beyond the 14 Å cutoff range. The arrows on the graphs point to RMSD values of residues that are in contact with the reactant complex or the transition state ("in contact" is defined as being within 3 Å of the center of mass of the reactant complex or transition state). Figure 6a shows the RMSD profiles of 1E9 with a water cap and no bound species. Note that the deviations of the residues are on the order of 0.3–0.6 Å, rather common for proteins. Residues in the binding pocket and remote from it display similar motions. Figure 6b shows the motion during dynamics of the 1E9–reactant complex. Here the motions of many residues are reduced, presumably due to the relatively tight fit of the reactant complex in the binding site of 1E9. The motions of the residues in contact with the reactant complex are especially damped, except for Leu H47. Such restrictions are entropically unfavorable, but are compensated for by the stabilizing interactions involving the binding-site residues and the reactant complex. Leu H47 and several other residues that are not in contact with the reactants have RMSD values of 0.25–0.48 Å. Figure 6c is a similar plot for the 1E9–transition-state complex. The motions here are similar to those involving the reactant complex. Figure 6d shows the changes between motions in the reactant complex and the transition state. The major changes in the residues in contact

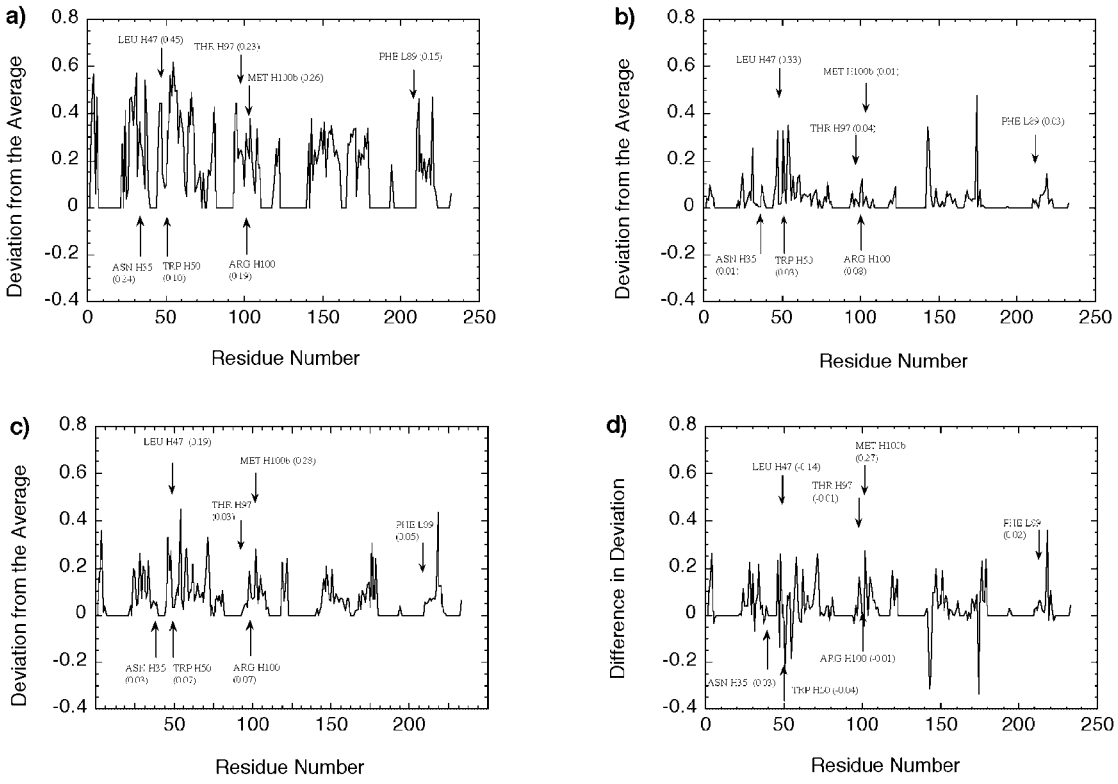

Figure 6. *Residue RMSD profiles derived from MD trajectories. a) Free antibody with water cap. b) Ground state complexed with 1E9. c) Transition state complexed with 1E9. d) Difference between b) and c). In all three figures a) – c), the horizontal axis corresponds to the amino acid sequence, the vertical axis gives the residue RMSD value in Å. Binding-site residues are labeled and indicated by arrows.*

with the transition state involve the reduced motions of the Leu H47 and increased motions of the Met H100b residues, both of which are in the vicinity of the SO_2 group of the diene. The SO_2 group moves significantly as the reactant complex changes to the transition state. The increase in the binding energy results in part from the antibody motions that respond to the change in geometry and electrostatic potential of the bound species, and cause increased contacts and electrostatic interactions. There are also some increases and decreases in motions of residues that are not in contact with the transition state. These residues are 5 – 14 Å away from the active site, so their role in catalysis, if any, is uncertain.

Conclusion

Antibody 1E9 is characterized by a hydrophobic pocket and one strategically placed polar residue. Our theoretical study indicates that the 1E9-catalyzed reaction proceeds through an *endo* pathway. The catalytic efficiency of 1E9 is achieved by the enthalpic stabilization of the transition state, which arises from the high shape complementarity between the antibody binding site and the transition state, as well as the better electrostatic interaction with the transition state than with the reactants.

We are grateful to the National Science Foundation for financial support of this research in the U.S., to Novartis Pharma AG for research in Switzerland, and to the National Center for Supercomputing Applications, University of Illinois at Urbana-Champaign, and the UCLA Office of Academic Computing for computational resources. We also thank Kinya Hotta for the preparation of the illustrations.

[1] U. Pindur, G. Lutz, C. Otto, *Chem. Rev.* **1993**, *93*, 741.
[2] S. Laschat, *Angew. Chem.* **1996**, *108*, 313; *Angew. Chem. Int. Ed. Engl.* **1996**, *35*, 289.
[3] R. A. Lerner, S. J. Benkovic, P. G. Schultz, *Science* **1991**, *252*, 659.
[4] P. G. Schultz, R. A. Lerner, *Science* **1995**, *269*, 1835.
[5] a) D. Hilvert, *Annu. Rev. Biochem.* **2000**, *69*, 751; b) D. Hilvert, *Top. Stereochem.* **1999**, *22*, 83.
[6] H. Oikawa, T. Kobayashi, K. Katayama, Y. Suzuki, A. Ichihara, *J. Org. Chem.* **1998**, *63*, 8748.
[7] D. Hilvert, K. W. Hill, K. D. Nared, M.-T. M. Auditor, *J. Am. Chem. Soc.* **1989**, *111*, 9261.
[8] a) J. Xu, Q. Deng, J. Chen, K. N. Houk, J. Bartek, D. Hilvert, I. A. Wilson, *Science* **1999**, *286*, 2345; b) For the study of a related Diels – Alder reaction catalyzed by 13G5, see: A. Heine, E. A. Stura, J. T. Yli Kauhaluoma, C. S. Gao, Q. L. Deng, B. R. Beno, K. N. Houk, K. D. Janda, I. A. Wilson, *Science* **1998**, *279*, 1934.
[9] M. J. Frisch, G. W. Trucks, H. B. Schlegel, P. M. W. Gill, B. G. Johnson, M. A. Robb, J. R. Cheeseman, T. A. Keith, G. A. Petersson, J. A. Montgomery, K. Raghavachari, M. A. Al-Laham, V. G. Zakrzewski, J. V. Ortiz, J. B. Foresman, J. Cioslowski, B. B. Stefanov, A. Nanayakkara, M. Challacombe, C. Y. Peng, P. Y. Ayala, W. Chen, M. W. Wong, J. A. Andres, E. S. Replogle, R. Gomperts, R. L. Martin, D. J. Fox, J. S. Brinkley, D. J. Defrees, J. Bakwe, J. P. Stewart, M. Head-Gordon, C. Gonzalez, J. A. Pople, *Gaussian 94*, Gaussian Inc., Pittsburgh, PA, **1995**.
[10] G. M. Morris, D. S. Goodsell, R. S. Halliday, R. Huey, W. E. Hart, R. K. Below, A. J. Olson, *J. Comput. Chem.* **1998**, *19*, 1639.
[11] B. H. Besler, K. M. Merz, P. A. Kollman, *J. Comput. Chem.* **1990**, *11*, 431.
[12] a) J. Åqvist, C. Medina, J. E. Samuelsson, *Protein Eng.* **1994**, *7*, 385; b) F. S. Lee, Z. T. Chu, M. B. Bolger, A. Warshel, *Protein Eng.* **1992**, *5*, 215 – 228; c) H. A. Carlson, W. L. Jorgensen, *J. Phys. Chem.* **1995**, *99*, 10667.
[13] J. Åqvist, S. M. Mowbray, *J. Biol. Chem.* **1995**, *270*, 9978.
[14] J. Åqvist, *J. Comput. Chem.* **1996**, *17*, 1587.
[15] J. Chen, R. Wang, K. N. Houk, M. Taussig, unpublished results.
[16] M. R. Haynes, M. Lenz, M. J. Taussig, I. A. Wilson, D. Hilvert, *Isr. J. Chem.* **1996**, *36*, 151.
[17] D. A. Pearlman, D. A. Case, J. W. Caldwell, W. S. Ross, T. E. Cheatham III, D. M. Ferguson, G. L. Seibel, U. C. Singh, P. K. Weiner, P. A. Kollman, *AMBER 4.1*, University of California, San Francisco, **1995**.
[18] J. H. Arevalo, M. J. Taussig, I. A. Wilson, *Nature* **1993**, *365*, 859.
[19] M. I. Page, W. P. Jencks, *Gazz. Chim. Ital.* **1987**, *117*, 455.
[20] J. Hine, *J. Am. Chem. Soc.* **1971**, *93*, 3701.
[21] J. Hermans, L. Wang, *J. Am. Chem. Soc.* **1997**, *119*, 2707.
[22] a) V. K. Misra, J. L. Hecht, A. S. Yang, B. Honig, *Biophys. J.* **1998**, *75*, 2262; b) B. Kuhn, P. A. Kollman, *J. Am. Chem. Soc.* **2000**, *122*, 2586, and references therein.
[23] A. Warshel in *Computer Modeling of Chemical Reactions in Enzymes and Solutions*, Wiley, New York, **1991**.

Received: April 25, 2000 [F 49]